The Korean Journal of Rheology,
Vol. 10, No. 4, December 1998 pp. 247-255

<연구논문>

이축 압출기를 이용한 혼련에서 삼성분계 블렌드의 상구조 형성과정

김형수† · 이시춘* · D.Y. Yu** · C.G. Gogos**
단국대학교 화학공학과
*삼성화학소그룹 종합연구소
**Polymer Processing Institute at Stevens Institute of Technology
(1998년 10월 29일)

Evolution of Phase Morphology During Compounding of Ternary Blends in a Twin Screw Extruder

Hyungsu Kim†, Shi-Choon Lee*, D.Y. Yu and C.G. Gogos****
Department of Chemical Engineering, College of Engineering, Dankook University
San 8 Hannam-Dong, Yongsan-Gu, Seoul, 140-714, Korea
*R&D Center, Chemicals Division, Samsung Chemical Group
332-2 Gochun-Dong, Euiwang-Shi, Kyoungki-Do, 437-010, Korea
**Polymer Processing Institute at Stevens Institute of Technology
Castle Point on the Hudson
Hoboken, NJ, 07030, USA
(Received October 29, 1998)

요 약

이축 압출기에서 삼성분계 블렌드가 용융 혼련될 때 상구조의 형성과정에 대하여 연구하였다. 삼성분계 블렌드의 연속상은 polycarbonate(PC)로 고정하였고 나머지 분산상을 이루는 성분으로는 acrylonitrile-butadiene-styrene(ABS), methyl methacrylate-butadiene-ethyl acrylate(MBE), styrene-acrylonitrile(SAN) 공중합체, 그리고 poly(methyl methacrylate)(PMMA)를 사용하였다. 블렌드의 여러 가지 조성에 따라 최종 상구조는 현저한 차이를 보였고 특히 MBE와 PMMA의 경우는 각각 PC-SAN의 계면에 선택적으로 위치하였다. 삼성분계 고분자 블렌드의 상구조 형성과정은 성분간의 계면장력과 합체 현상의 상호 작용에 의하여 지배되었으며 합체의 정도는 계면에서의 점도에 의하여 민감하게 변화되었다.

Abstract—The morphological changes during melt compounding of ternary blends containing various combinations of acrylonitrile-butadiene-styrene(ABS), methyl methacrylate-butadiene-ethyl acrylate(MBE), styrene-acrylonitrile(SAN) copolymers, and poly(methyl methacrylate)(PMMA) as dispersed components in a fixed matrix of polycarbonate(PC) have been investigated. Depending on the composition of the blend, MBE particles and PMMA phase appear to locate at the PC-SAN interface under the influence of interfacial tensions and motion induced coalescence. The interfacial viscosity is found to be a critical factor that affects the amount of coalescence.
Key words: morphology development; blends;interfacial tension; coalescence

1. Introduction

Multicomponent polymer blends provide an effective route to expand the applicability of polymeric materials by satisfying the diversified needs in industrial utilization. Based on the high performance and attractive versatility, demand for such materials is expected to continuously grow [1]; and the best known members of the class include polycarbonate(PC)/acrylonitrile-butadiene-styrene(ABS), PC/poly(butylene terephthalate)(PBT)/methacrylated butadiene-styrene(MBS), and poly(phenylene ether)(PPE)/polyamide (PA)/styrenic block copolymer(SBC), etc.. These materials constitute the base resins for various parts in automotive and appliances and the major contributions of them are due to excellent impact strength, heat resistance and chemical resistance, which are not readily obtained by simple binary combination of the components included in the blends.

Since there are strong correlations between phase morphology and physical properties in polymer blends, it is of great importance to properly control and generate the

†Corresponding author

desired morphology. Moreover, as numerous polymers are joined by mechanical mixing, the interplay of each constituent becomes very sophisticated, making design of new blends more difficult. Fortunately, a simple and useful theory has been demonstrated by Hobbs et al. for the prediction of phase morphology in ternary blends[2]. By evaluating the spreading coefficient, λ_{ij}, defined by Harkin's equation in terms of component interfacial tensions, γ_{mn}'s :

$$\lambda_{31} = \gamma_{12} - \gamma_{32} - \gamma_{13} \quad (1)$$

it is possible to picture the resulting morphology a priori; i. e., depending on the positive or negative value of spreading coefficients, spreading behavior between two components or their separate dispersion is determined for a fixed matrix in a three phase system. The strong influence of spreading behavior on the phase morphology has been also verified in different multiphase polymer blends produced by twin screw extruder[3,4]. On the other hand, combining with Harkin's analysis, Cheng et al.[5] developed a rigorous surface free energy analysis which enables one to trace the locus of impact modifiers in the two-phase matrix. The prediction was made by evaluating the critical interfacial tension ratio: if the following condition is satisfied

$$-1 < \frac{\gamma_{13} - \gamma_{23}}{\gamma_{12}} < 1 \quad (2)$$

where γ_{ij} is the interfacial tension and the component 3 denotes the impact modifier particles distributed in the phases of the other components, the particles will be trapped at the 1-2 interface. More recently, a more rigorous and general theory has been developed by Guo et al.[6], which predicts the equilibrium phase structure of a multiphase system by analysing interfacial free energy. Obviously, such contributions provide a valuable milestone for designing new multicomponent polymeric materials; since, in particular, the location of impact modifier particles considerably affects the mechanical properties of the blends. In this study, a number of ternary blends composed of PC, poly(styrene-co-acrylonitrile)(SAN), poly (methyl methacrylate)(PMMA), ABS, and methyl methacrylate-butadiene-ethylacrylate(MBE) were examined. Based on appropriate combinations of available polymers, we were able to drive spreading behavior or entrapping of impact modifier particles at the interface of the mixed matrix. In fact, the blend systems employed here are analogous to those of previous studies[2,5] in which the major concern was focused on the equilibrium partitioning of each component in the whole blends. It is of particular interest of this study to explore the principal mechanism of spreading and entrapping behaviors during melt compounding of ternary blends in a twin screw extruder. Although a similar issue has been addressed in a paper by Dekkers et al.[3], where the migration of the predispersed impact modifier particles into PC phase or PC-polystyrene (PS) interface was detected, no direct observation was made on the evolution of spreading and entrapping behaviors in ternary blends. Therefore, this study is intended to elucidate the kinematics of morphology development in multiphase polymer blends.

2. Experimental

The materials used in this study are all commercially available polymers and their detailes are summarized in Table 1. MBE modifier is an emulsion-made core-shell elastomer available from Kurhea Chem. Co. as EXL-2602. It contains about 80% by weight of butadiene-ethyl

Table 1. Polymers used in this study

Polymer	Abbreviation	Source	Molecular weight	Copolymer composition
Polycarbonate	PC	Teijin (Panlite L1250W)	$\overline{M}n$=15,000 $\overline{M}w$=27,000	-
Poly(styrene-co-acrylonitrile)	SAN26	Cheil Ind. Inc.	$\overline{M}n$=91,000 $\overline{M}w$=170,000	26% AN
	SAN32	Cheil Ind. Inc.	$\overline{M}n$=56,000 $\overline{M}w$=120,000	32% AN
Poly(methyl methacrylate)	PMMA	LG Chemicals (IH 830)	$\overline{M}n$=37,000 $\overline{M}w$=79,000	-
Acrylonitrile-butadiene-styrene	ABS	Cheil Ind. Inc.		SAN grafted butadiene rubber(45% polybutadiene, 24% AN in free SAN)
Methyl methacrylate-butadiene-ethyl acrylate	MBE	Kurea Chem. Ind.		PMMA shell/butadiene-ethyl acrylate core(20/80)

acrylate rubber with 20% of PMMA outer shell. All the blends were compounded on the Twin Screw Mixing Element Evaluator(TSMEE) which retains the main geometric features of a Werner & Pfleiderer ZSK-30 co-rotating twin screw extruder. In addition to various useful features including on-line measurements of rheological property, pressure, and temperature, TSMEE offers a facilitated route for carcass experiments which are essential for the study of phase morphology development during melt compounding of polymer blends. The details of TSMEE is given elsewhere[7]. In each case, the components were first dry blended and fed simultaneously to the hopper at a rate of 36g/min using a loss-in-weight feeder. The barrel was maintained at a temperature of 250°C except the feed zone where the barrel temperature was set at 180°C. The screw speed was set at 120 rpm, which corresponds to an average shear rate of 326 sec^{-1}[7]. After reaching steady state, the machine was brought down to a stop. The device was then fast cooled by circulating cooling water to a temperature of 100°C to freeze the material. The time required for cooling was about 60 sec. after stopping. It is important for the study of morphology development to minimize the cooling time since melt blend morphology can change significantly during annealing at elevated temperature or slow cooling [8-12]. Within the accessible cooling time of this experiment, one might expect morphology change like breakup of elongated cylinder[12]. Nevertheless, the analysis given here should at least provide a reliable rationale based on the fixed sampling regime for all cases. After the cooling was completed, the barrel was opened and blend samples were taken along the length of the extruder. The extruded strands during the steady state operation were directly put into cold water to eliminate possible morphology change. The schematic illustration of configuration and sampling positions is shown in Fig. 1.

Fig. 1. Schematic illustration of screw configuration and sampling positions in TSMEE.

The morphology of the blends was characterized by transmission electron microscopy(TEM) using a Jeol JEM-2000EX. For improved contrast, two stage staining method was applied: First, specimen blocks broken from the carcass samples at liquid nitrogen temperature were stained in a 2% solution of OsO_4 for 48 hours. Ultrathin slices were cut using a Reichert-Jung Ultracut Microtome at room temperature. Then, the thin sections were further stained by the vapor of a 0.5% RuO_4 solution for 30 minutes[13]. Average domain sizes were calculated from SEM photomicrographs by using an image analyzer. Samples for SEM were sputter coated with a thin layer of Au and observations were made using a Jeol JSM-840A.

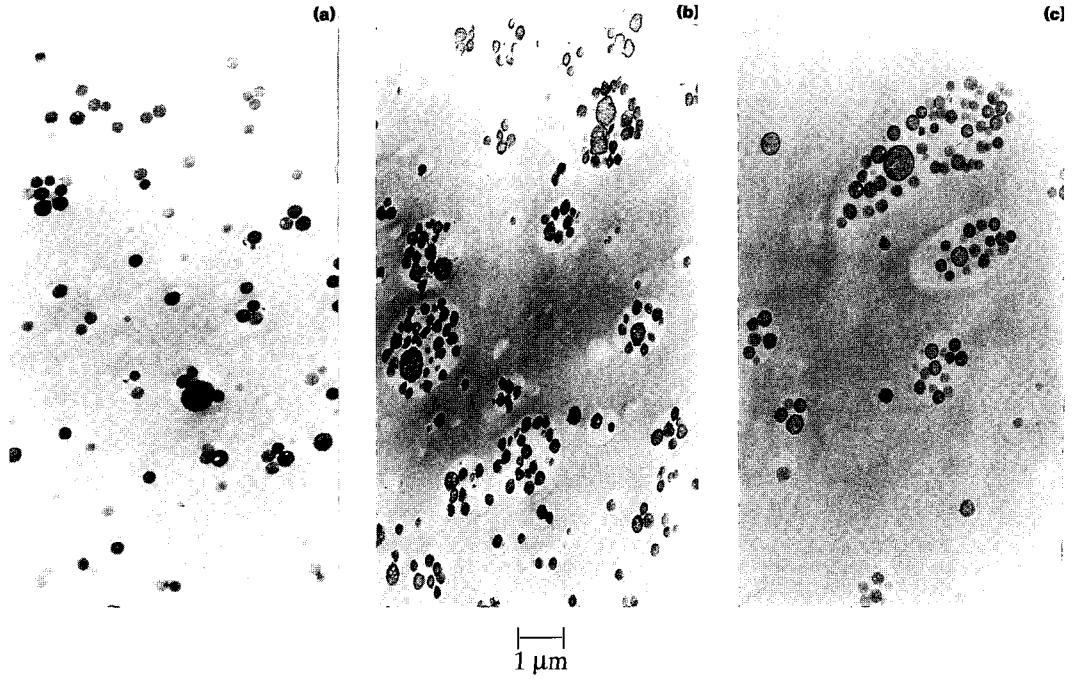

Fig. 2. TEM photomicrographs of PC/SAN26/ABS(85/10/5) blends for various sampling positions. (a) position 2, (b) position 4, (c) position 6

3. Results and Discussion

A remarkable variation of phase morphology for the various axial position of the extruder in the blend of PC/SAN26/ABS(85/10/5) is depicted by a series of TEM shown in Fig. 2. During the carcass sampling, it was found in most cases that softening and melting of all components in the blend were completed right after the first kneading section which is followed by the first sampling position shown in Fig. 1. As shown in Fig. 2(a), domains of SAN and ABS are uniformly dispersed with phase size of well below 1 μm. Most of the ABS particles appear to be incorporated into the SAN phase; while many SAN particles remain unoccupied by ABS. It is noteworthy that the size reduction occurred very fast at the front section of kneading blocks. Such rapid breakup phenomenon of minor phase in polymer blends relates to the underlying mechanism for initial morphology development proposed by Scott and Macosko[14]. According to their study, the major reduction in domain size occurs at the early stage of melting of softening along with the sequential formation of sheet, lace, cylinder and droplets. In our previous study[15], analogous mode of breakup mechanism has been confirmed in PC/SAN blends. As the axial position moves to the die region, the initially well dispersed domains of ABS and SAN are getting close together(Fig. 2(b)) and finally forms a typical morphology of commercial PC/ABS blend having phase sizes of more than 1 μm(Fig. 2(c)). The morphology development of PC/SAN32/MBE(85/10/5) system is shown in Fig. 3, where the progress has been made in a similar fashion with Fig. 2 except the locus of impact modifier particles. From the surface energy analysis given by Cheng et al.[5], the MBE particles are predicted to locate at the PC-SAN32 interface, whereas ABS particles are expected to reside in SAN phase. Each case is experimentally confirmed in Fig. 2(c) and 3(c), respectively. Fig. 3 offers a useful information on tracing the movement of impact modifiers with various modes of phase structure. After the fine dispersion of SAN and MBE particles(Fig. 3(a)), it is observed in Fig. 3(b) that MBE particles are getting agglomerated(arrow 1) or entering the border of SAN phase which was already enlarged by the coalescence of several smaller SAN domains(arrow 2), thus forming premature dual-phase domains. In addition, these dual-phase domains appear to be combined(arrow 3) to promote the ultimate phase morphology shown in Fig. 3(c). Note that the domain size of SAN is further increased and all of the MBE particles are located at PC-SAN interface with partial agglomerations. The incomplete coverage of SAN phase may be due to these agglomerations and/or the insufficient amount of MBE to cover the entire interfacial area between PC and SAN.

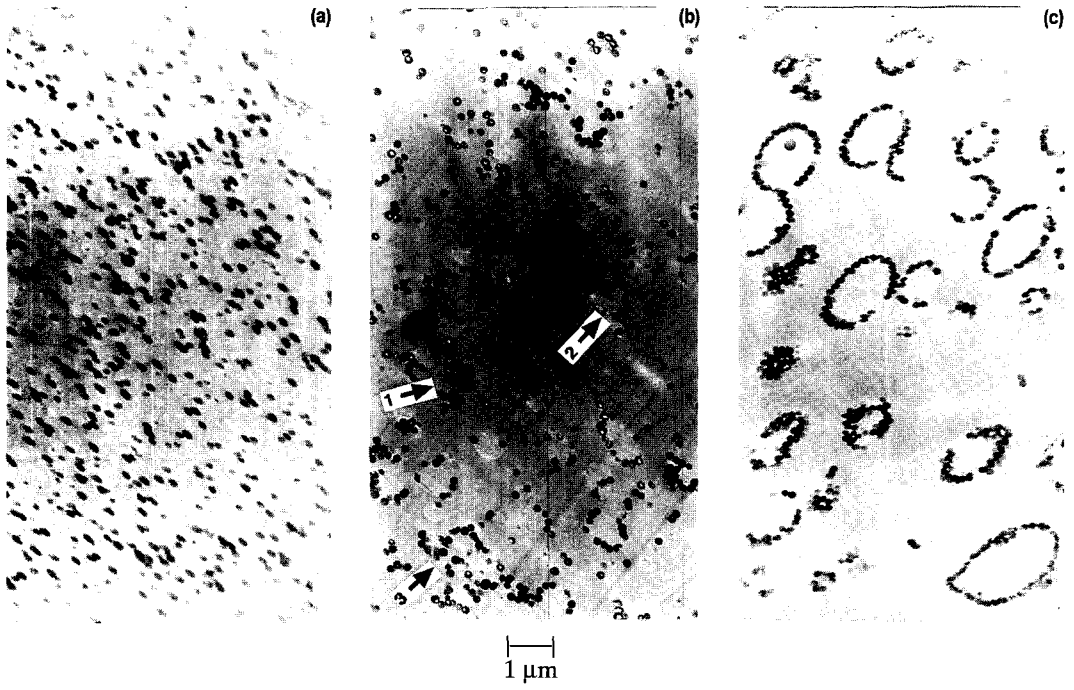

Fig. 3. TEM photomicrographs of PC/SAN32/MBE(85/10/5) blends for various sampling positions. (a) position 2, (b) position 4, (c) position 6

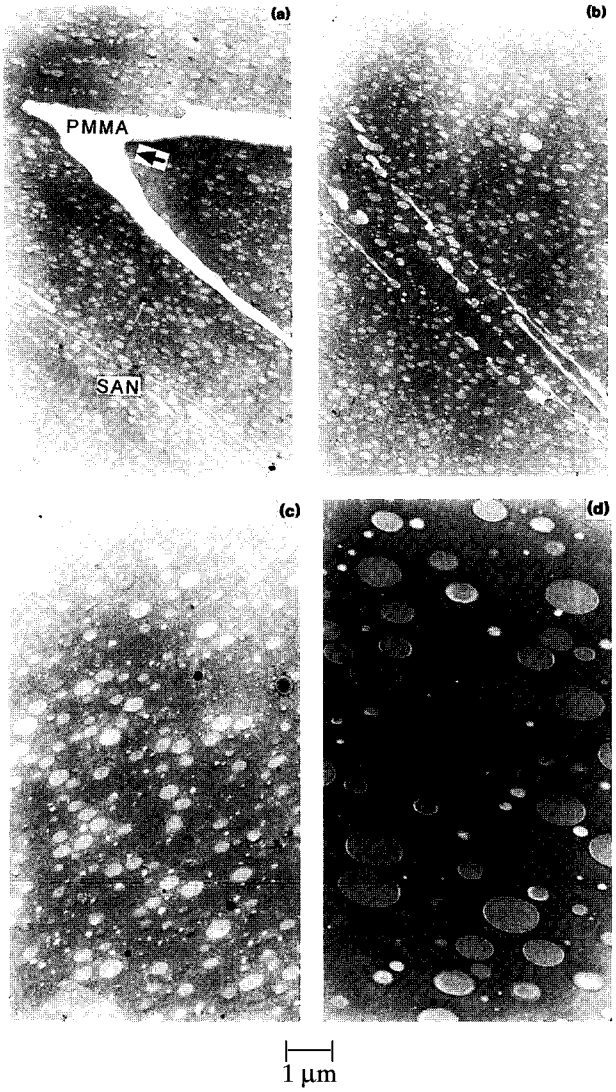

Fig. 4. TEM photomicrographs of PC/SAN32/PMMA(85/10/5) blends for various sampling positions. (a),(b) position 1, (b) position 3, (c) position 5(Tiny white spots stand for PMMA phase)

The changes in phase morphology during extrusion is even more striking in ternary blend without impact modifier. Fig. 4 represents the case of PC/SAN32/PMMA (85/10/5) in which, based on the evaluation of the spreading coefficient with previously reported interfacial tension data[16], positive spreading behavior of PMMA on SAN32 is expected. The pictures taken from different spots of sampling position 1(Fig. 4(a), 4(b)) shows that majority of SAN(grey) and PMMA(white) phases are dispersed as particulates in the PC(dark grey) phase, while the other part of the phases are still in the course of deformation and stretching to form cylinders or threads which eventually break up into droplets via Rayleigh-type instabilities[17-19]. In terms of the apparent size of the dispersed phases, PMMA phase appears as extremely tiny particles compared to SAN phase. This might be expected since the interfacial tension of PC/PMMA is lower than that of PC/SAN32(1.96 dyne/cm vs. 4.0 dyne/cm at 200°C [16]) and furthermore PC/PMMA blend has been reported to be nearly miscible[20-22]. Accordingly, during the continuous extension of minor phases of sheet or lace structure, the pair having more favorable interaction would in principle provide more slender threads, i.e., larger surface to volume ratio, which in turn results in droplets of reduced size. Of course, at the early stage of melt-mixing, where affine deformation of the minor phase prevails with large capillary number, interfacial forces cannot resist the stresses imposed by the flow field in an extruder; however, once sufficient decrease in local radii of threads(order of 1 μm) is achieved, the interfaces should become active especially in relatively low stress region[23] and breakup initiates simply because the interfacial tension tends to minimize the interface between the two phases. It is pointed out in Fig. 4(a) that the elongated PMMA phase is experiencing a folding action (see arrow) rendering efficient generation of large interfacial area within the limited residence time. Such stretching and folding operations are basically provided by kneading elements in a twin screw extruder[24], which are responsible for the formation of fully elongated threads and consequently the fast dispersion of the minor phase along with the breakup mechanisms mentioned earlier. It is also emphasized that alternative level of high and low stresses are available in kneading blocks due to the cyclic movements of compression and expansion, which also greatly enhances the effectiveness of dispersion process [25]. In fact, according to Tomotika's analysis[18], it is critical to develop the thinnest possible threads in a given mixing environment; since the required breakup time is proportional to the thread diameter. Regarding the estimation of breakup time, Sundararaj et al.[12] suggested that much faster breakup(order of few seconds) than the original prediction by Tomotika's analysis is possible due to the significantly larger initial distortion which is mainly caused by polymer memory effects. Similar argument is pertinent here and comparable order of breakup time was obtained by assuming initial distortion of 25 nm for a thread of SAN in PC matrix. It is interesting to note that some of SAN particles are resided in the extended PMMA phase as shown in Fig. 4(a). Moreover, a peculiar morphology is represented in Fig. 4(b) where PMMA enveloped SAN particles are

generated from thin threads of PMMA containing SAN droplets via Rayleigh-type instabilities. It is tempting to attribute these observations to the miscibility between PMMA and SAN32 since PMMA and SAN are reported to be miscible for AN contents between 9 and 33 wt%[25-31]. However, PMMA particles were hardly found in SAN phase vice versa and complicated spacial distribution of components in solid or solid-melt transition state may be interrelated. Accordingly, the phenomenon is recognized as a localized one and no further interpretation is made.

In position 3, on the other hand, threads of SAN or PMMA phase are not found indicating the breakup process has been completed(Fig. 4(c)). Each of the SAN and PMMA domains is dispersed apart with somewhat increased particle sizes compared to those in position 1. The expected spreading behavior is illustrated in Fig. 4(d). Here SAN domains are surrounded by thin layer of PMMA phase and domains of pure PMMA which will eventually spread over the other SAN are also found. Although the exact place of complete envelope formation and its more detailed progress are not displayed, it is clearly seen from these morphological findings that again, considerable coalescence between the dispersed phases, presumably following similar modes described in PC/SAN 32/MBE system, took place during the course of envelope formation. Note that the phases have been continuously enlarged along with the axial position of the extruder ever since the breakup of elongated threads occurred.

The common features identified from the foregoing results emphasize the fact that the morphology development in ternary blends accompanies coalescence of discrete domains which are mostly produced during the initial softening and melting stage. The coalescence in immiscible polymer blends has been the subject of numerous studies performed at static[9-11,32-36] or flow conditions[37-40], and several theories have been developed to interpret the coalescence effect[41-47]. Although various kinematic models were also proposed to predict the domain sizes in polymer blends, discrepancies are still inevitable due to the polymer viscoelasticity and

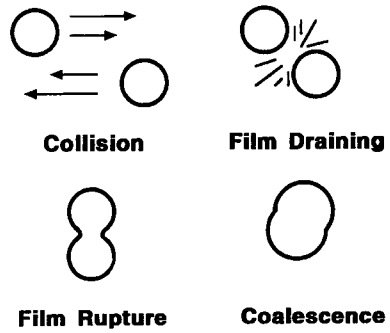

Fig. 5. Idealized depiction of shear-induced coalescence of dispersed Newtonian droplets(adapted from ref.36).

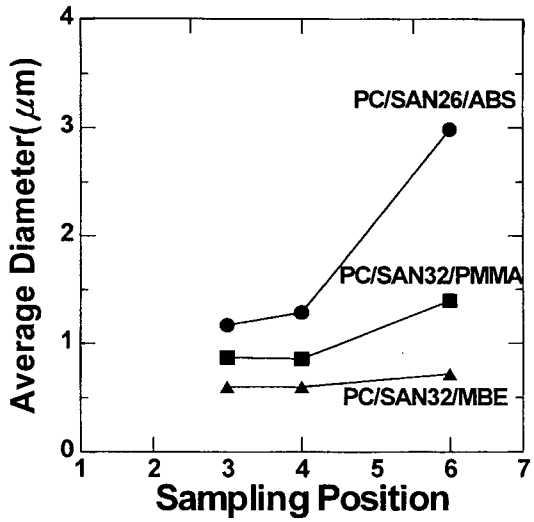

Fig. 6. Average phase size as a function of sampling position(Blend ratio was fixed as 85/10/5).

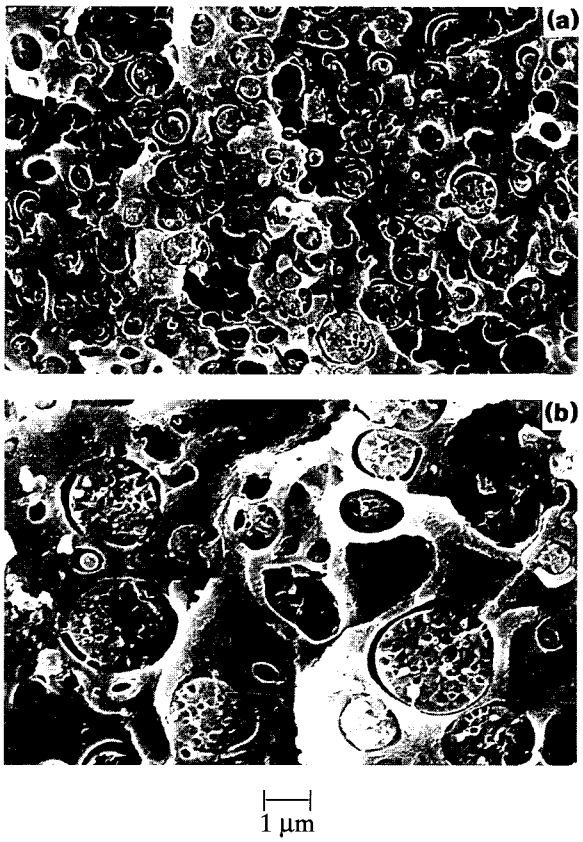

Fig. 7. SEM photomicrographs of PC/SAN26/ABS(85/10/5) blend. (a) position 3, (b) position 6

complexity of the given flow field during melt-mixing. On the other hand, qualitative aspects of flow induced coalescence in polymer blends are rather well described by a three-step mechanism[48] originally modeled for Newtonian liquid drops. A schematic diagram of the mechanism is reproduced in Fig. 5. Here, the droplets are brought close together by the flow field, and then the matrix film between the drops thins until the interface ruptures and then coalescence occurs. Of course the nature of the whole process in polymeric systems may be quite different from that of Newtonian liquid drops; however, the collision of domains and removal of matrix phase should be maintained for both cases as a prerequisite for coalescence. Furthermore, considering the high viscosity of polymer melt, drainage of the matrix film is the rate-determining step[49]; hence, the amount of coalescence should be decreased by increasing matrix viscosity[37,42]. In addition, the influence of interfacial viscosity on coalescence effect should be addressed, because highly entangled chains of domain and matrix with favorable interactions or copolymers formed by in situ reactions at the interface, thus increasing the interfacial viscosity, would in principle retard coalescence by limiting the drainage of matrix fluid. Fig. 6 summarizes the changes in the phase size of each blend as a function of sampling position. It shows that the phase sizes of PC/SAN26/ABS and PC/SAN32/PMMA are significantly increased as approaching the dieout position, whereas PC/SAN32/MBE blend represents the least increment of phase size among the blends under consideration. The trends shown in Fig. 6 parallel the notion that the interfacial viscosity controls the amount of coalescence in a fixed matrix. In PC/SAN 32/MBE blend, the interfacial viscosity is expected to be much higher than in the other two cases owing to the presence of viscous MBE particles at PC-SAN interface. Since such viscous shell formation is not available in PC/SAN26/ABS and PC/SAN32/PMMA, these blends are more apt to experience coalescence by facilitating the drainage of matrix film. From the point of variation in the interfacial tension, addition of either MBE or PMMA into PC/SAN32 blend reduces the interfacial tension of the system by locating at the interface; however, final phase size is two or three times larger in PC/SAN32/PMMA system with broader size distribution. This comparison

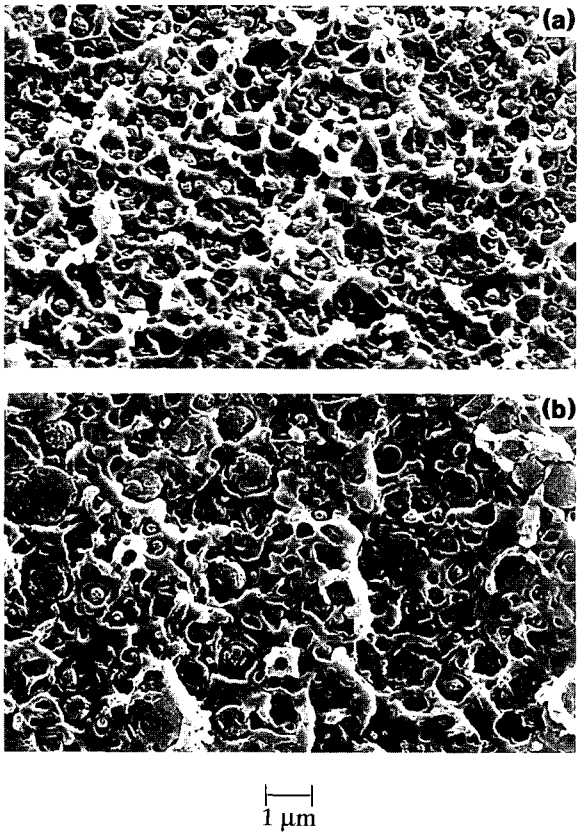

Fig. 8. SEM photomicrographs of PC/SAN32/MBE(85/10/5) blend. (a) position 3, (b) position 6

Fig. 9. SEM photomicrographs of PC/SAN32/PMMA(85/10/5) blend. (a) position 3, (b) position 6

emphasizes the fact that steric stabilization at the interface is more important than simply reducing the interfacial tension in minimizing the amount of coalescence as proposed by Sundararaj and Macosko[38]. An analogous result on the decreased coalescence by core-shell impact modifier in PC/SAN blend has been reported by Debier et al.[34] from the annealing experiment. SEM photomicrographs of each blend for selected sampling positions are presented in Fig. 7, 8 and 9, respectively. A dramatic change of phase size is observed in PC/SAN26/ABS(Fig. 7(b)) and PC/SAN32/PMMA(Fig. 9(b)) as plotted in Fig. 6. Note in Fig. 9(b) that two or three domains are coalescing in a row(see arrows).

Conclusions

The evolution of phase morphology in ternary blends appears to be strongly influenced by the coalescence of individual dispersed phase. While the phase size of each domain at the early stage of melt-mixing is in the minimum range throughout the whole compounding process, subsequent coalescence increases domain size of each phase and leads to the formation of dual phase domains. As expected by the available surface free energy analysis, MBE particles and PMMA phases were located at PC-SAN32 interface, whereas ABS particles were resided in SAN26 phase. In the later stage until the exit of the extruder, coalescence is further promoted in various amounts depending on the nature of dual phase morphology. Viscous shell formation of MBE particles at the interface of PC-SAN32 suppressed the coalescence effect due to the increased interfacial viscosity. It is concluded that the domain sizes and phase structure of ternary blends are determined by the interplay of interfacial tensions and motion induced coalescence.

Acknowledgement

The present research was conducted by research fund of Dankook university.

References

1. L.A. Utracki, *Polym. Eng. Sci.*, **35**, 2 (1995).
2. S.Y. Hobbs, M.E.J. Dekkers, and V.H. Watkins, *Polymer*, **29**, 1598 (1988).
3. M.E.J. Dekkers, S.Y. Hobbs, I. Bruker, and V.H. Watkins, *Polym. Eng. Sci.*, **30**, 1628 (1990).
4. M.E.J. Dekkers, S.Y. Hobbs, and V.H. Watkins, *Polymer*, **32**, 2150 (1991).
5. T.W. Cheng, H. Keskkula, and D.R. Paul, *Polymer*, **33**, 1606 (1992).
6. H.F. Guo, S. Packirisamy, N.V. Gvozdic, and D.J. Meier, *Polymer*, **38**, 785(1997).
7. C.G. Gogos, M. Esseghir, D.Y. Yu, D.B. Todd, and J.E. Curry, SPE ANTEC Tech. *Papers*, **40**, 270 (1994).
8. U. Sundararaj, C.W. Macosko, R.J. Rolando, and H.T. Chan, *Polym. Eng. Sci.*, **32**, 1884 (1992).
9. D. Quintens, G. Groeninckx, M. Guest, and L. Aerts, *Polym. Eng. Sci.*, **30**, 1474 (1990).
10. D. Quintens, G. Groeninckx, M. Guest, and L. Aerts, *Polym. Eng. Sci.*, **30**, 1484 (1990).
11. T.W. Cheng, H. Keskkula, and D.R. Paul, *J. Appl. Poly. Sci.*, **45**, 1245 (1992).
12. U. Sundararaj, C.W. Macosko, A. Nakayama, and T. Inoue, *Polym. Eng. Sci.*, **35**, 100 (1995).
13. J.S. Trent, J.I. Scheinbeim, and Couchman, P.R., *Macromolecules*, **16**, 589 (1983).
14. C.E. Scott and C.W. Macosko, *Polymer*, **36**, 461 (1995).
15. S.C. Lee, H. Kim, S.S. Woo, D.Y. Yu, S.H. Kim, M. Esseghir, and C.G. Gogos, Proceeding of 11th Polymer Processing Society Meeting, March 27-30, 223 (1995).
16. V.H. Watkins and S.Y. Hobbs, *Polymer*, **34**, 3955 (1993).
17. Lord Rayleigh, *Proc. R. Soc.*, **29**, 71 (1879).
18. S. Tomotika, *Proc. R. Soc.*, **A150**, 332 (1935).
19. P. Elemans, J.H.M. Janssen, and H.E.H. Meijer, *J. Rheol.*, **34**, 1311 (1990).
20. M. Nishimoto, H. Keskkula, and D.R. Paul, *Polymer*, **32**, 1274 (1991).
21. K.E. Min and D.R. Paul, *J. Appl. Polym. Sci.*, **37**, 1153 (1989).
22. J.M. Saldanha and Y. Kyu, *Macromolecules*, **20**, 2840 (1987).
23. H.E.H. Meijer and J.M.H. Janssen , Mixing and Compounding of Polymers, I. Manas-Zloczower and Z. Tadmor, Ed., Hanser Publishers, New York, 1994, Chapter 4.
24. D. Todd, Two-Phase Polymer Syatems, L.A. Utracki, Ed., Hanser Publishers, New York, 1991, Chapter 3.
25. H.P. Grace, *Chem. Eng. Commun.*, **14**, 225 (1982).
26. M.E. Fowler, H. Keskkula, and D.R. Paul, *Polymer*, **28**, 1703 (1987).
27. V.D.J. Stein, R.H. Illers, and H. Henders, *Angew. Makromol. Chem.*, **36**, 89 (1974).
28. R.E. Bernstein, C.A. Cruz, D.R. Paul, and J.W. Barlow, *Macromolecules*, **10**, 681 (1977).
29. K. Naito, G.E. Johnson, D.L. Allara, and T.K. Kwei, *Macromolecules*, **11**, 1260 (1978).
30. M.E. Fowler, J.W. Barlow, and D.R. Paul, *Polymer*, **28**, 1177 (1987).
31. M.E. Fowler, J.W. Barlow, and D.R. Paul, *Polymer*, **28**, 2145 (1987).
32. M.P. Lee, A. Hiltner, and E. Baer, *Polymer*, **33**, 675 (1992).
33. M.P. Lee, A. Hiltner, and E. Baer, *Polymer*, **33**, 685 (1992).
34. D. Debier, J. Devaux, R. Legras, and D. Leblance, *Polym. Eng. Sci.*, **34**, 613 (1994).
35. B. Crist and A.R. Nesarikar, *Macromolecules*, **28**, 890 (1995).
36. D.W. Park and R.J. Roe, *Macromolecules*, **24**, 5324 (1991).
37. C.M. Roland and G.G.A. Bhm, *J. Polym. Sci.*, **22**, 79 (1984).
38. U. Sundararaj and C.W. Macosko, *Macromolecules*, **28**, 2647 (1995).
39. A.P. Plochocki, S.S. Dagli, R.D. Angrew, *Polym. Eng. Sci.*, **30**,

741 (1990).
40. M.A. Huneault, Z.H. Shi, and L.A. Utracki, *Polym. Eng. Sci.,* **35**, 115 (1995).
41. J.J. Elmendorp and A.K. Van Der Vegt, *Polym. Eng. Sci.,* **26**, 1332 (1986).
42. I. Fortelný and J. Kovář, *Polym. Compos.,* **9**, 119 (1988).
43. J.G.M. Van Gibergen and H.E.H. Meijer, *J. Rheol.,* **35**, 63 (1991).
44. R.K. Chesters, *Trans. Inst. Chem. Eng. (A)* **69**, 259 (1991).
45. G. Marrucci, *Chem. Eng. Sci.,* **24**, 975 (1969).
46. I. Fortelný and A. živný, *Polymer,* **36**, 4113 (1995).
47. N. Tokita, *Rubber Chem. Technol.,* **50**, 292 (1977).
48. R.S. Allan and S.G. Mason, *Trans. Faraday Soc.,* **57**, 2027 (1961).
49. J.J. Elmendorp, Mixing in Polymer Processing, C. Rauwendaal, Ed., Marcel Dekker, Inc., New York, 1991, Chapter 2.